Dysfunction of the circadian clock in the kidney tubule leads to enhanced kidney gluconeogenesis and exacerbated hyperglycemia in diabetes

OPEN

Camille Ansermet[1,6], Gabriel Centeno[1,6], Yohan Bignon[1,6], Daniel Ortiz[2,6], Sylvain Pradervand[3], Andy Garcia[1], Laure Menin[2], Frédéric Gachon[1,4], Hikari AI. Yoshihara[5] and Dmitri Firsov[1]

[1]*Department of Biomedical Sciences, University of Lausanne, Lausanne, Switzerland;* [2]*Mass Spectrometry Service, Institute of Chemical Sciences and Engineering, Ecole Polytechnique Fédérale de Lausanne, Lausanne, Switzerland;* [3]*Genomic Technologies Facility, University of Lausanne, Lausanne, Switzerland;* [4]*Institute for Molecular Bioscience, The University of Queensland, Queensland, Australia; and* [5]*Institute of Physics, Ecole Polytechnique Fédérale de Lausanne, Lausanne, Switzerland*

The circadian clock is a ubiquitous molecular time-keeping mechanism which synchronizes cellular, tissue, and systemic biological functions with 24-hour environmental cycles. Local circadian clocks drive cell type- and tissue-specific rhythms and their dysregulation has been implicated in pathogenesis and/or progression of a broad spectrum of diseases. However, the pathophysiological role of intrinsic circadian clocks in the kidney of diabetics remains unknown. To address this question, we induced type I diabetes with streptozotocin in mice devoid of the circadian transcriptional regulator BMAL1 in podocytes (cKOp mice) or in the kidney tubule (cKOt mice). There was no association between dysfunction of the circadian clock and the development of diabetic nephropathy in cKOp and cKOt mice with diabetes. However, cKOt mice with diabetes exhibited exacerbated hyperglycemia, increased fractional excretion of glucose in the urine, enhanced polyuria, and a more pronounced kidney hypertrophy compared to streptozotocin-treated control mice. mRNA and protein expression analyses revealed substantial enhancement of the gluconeogenic pathway in kidneys of cKOt mice with diabetes as compared to diabetic control mice. Transcriptomic analysis along with functional analysis of cKOt mice with diabetes identified changes in multiple mechanisms directly or indirectly affecting the gluconeogenic pathway. Thus, we demonstrate that dysfunction of the intrinsic kidney tubule circadian clock can aggravate diabetic hyperglycemia via enhancement of gluconeogenesis in the kidney proximal tubule and further highlight the importance of circadian behavior in patients with diabetes.

Correspondence: *Hikari AI Yoshihara, Institute of Physics, Ecole Polytechnique Fédérale de Lausanne, Lausanne, Switzerland; or Dmitri Firsov, Department of Biomedical Sciences, University of Lausanne, 27 rue du Bugnon, 1005 Lausanne, Switzerland. E-mail: hikari.yoshihara@epflu.ch or dmitri.firsov@unil.ch*

[6]CA, GC, YB, and DO contributed equally to this work.

Received 28 June 2021; revised 1 November 2021; accepted 9 November 2021; published online 25 November 2021

Kidney International (2022) **101,** 563–573; https://doi.org/10.1016/j.kint.2021.11.016

KEYWORDS: circadian clock; diabetes; gluconeogenesis; proximal tubule

Translational Statement

In diabetes, the kidney contributes to the development of diabetic hyperglycemia by increasing glucose reabsorption from primary urine and by upregulating gluconeogenesis in the proximal tubule. However, these 2 processes are also controlled by the circadian clock, a mechanism that synchronizes a variety of specific kidney functions with daily light–dark cycles. Herein, we demonstrate that dysfunction of the intrinsic circadian clock in the renal tubule can aggravate diabetic hyperglycemia via enhancement of renal gluconeogenesis. These results highlight the importance of circadian effects in diabetic patients, with potential implications for glucose management.

Diabetes is a systemic disease in which the kidney plays a particular role. In diabetes, the kidney contributes to the development of diabetic hyperglycemia by increasing glucose reabsorption from the primary urine[1] and by enhancing glucose production via gluconeogenesis.[2,3] However, long-term elevation of blood glucose levels may, in turn, cause diabetic nephropathy (DN), one of the most serious complications of diabetes, characterized by glomerular, tubular, and vascular damage in the kidney. Although metabolic stress is the primary factor involved in pathogenesis and progression of DN, hyperglycemia alone does not lead to kidney insufficiency in most diabetic patients.[4] This suggests that combination with an intercurrent illness or presence of environmental, genetic, or epigenetic "second hits" may be required for initiation and/or accelerated progression of DN.

Recent research has suggested that the circadian clock mechanism is at the intersection of several (patho)physiological processes in the kidney.[5] Conditional perturbation of

the circadian clock in different renal cell types in animal models results in the disruption of circadian rhythms in glomerular filtration rate (GFR),[6] partial loss of blood pressure control,[7,8] substantial alterations in renal metabolic pathways,[9,10] and accelerated progression of chronic kidney disease.[11] In humans, shift work-related circadian misalignment between the biological clock and feeding and activity rhythms is associated with decreased GFR,[12] increased urinary albumin excretion,[13] nocturia and increased kidney urine production,[14] and increased risk of chronic kidney disease.[15]

Interestingly, the circadian clock in the kidney controls, or is interconnected with, many cellular pathways that are involved in the pathogenesis of diabetes and/or DN. For instance, renal tubule-specific knockout of the transcriptional activator BMAL1 (also named ARNTL), a central element of the circadian clock machinery, results in a marked increase in expression levels of mRNAs encoding proteins involved in renal glutamine gluconeogenesis, including glutamine transporter SNAT3 (SLC38A3), glutaminase (GLS), and glutamate dehydrogenase 1 (GLUD1).[9] More important, these expression changes occur in normoglycemic knockout animals. Solocinski *et al.* have demonstrated that the circadian clock protein PER1 is involved in the transcriptional regulation of glucose transporter *Sglt1* (*Slc5a1*) in proximal tubule cells,[16] and Ansermet *et al.* have shown that the circadian clock in podocytes controls expression of the *Arhgap24* gene associated with predisposition to DN in both type 1 and type 2 diabetes.[6] Both high glucose levels and tubular deficiency of BMAL1 have been shown to strongly induce expression of cyclin-dependent kinase inhibitor $p21^{CIP1}$ (*Cdkn1a*), a critical factor in triggering cellular senescence in the diabetic kidney.[9,17] The nicotinamide adenine dinucleotide–dependent deacetylase sirtuin 1 (SIRT1), one of the key regulators of podocyte damage in DN,[18] has been identified as a master regulator of the energy feedback loop within the core clock network.[19] Another cellular mechanism that links DN with the circadian clock is the mammalian target of rapamycin, a kinase that coordinates cellular metabolism with circadian time-keeping.[20] Altered mammalian target of rapamycin signaling has also been recognized as an important pathogenic factor in diabetes-induced damage of renal tubular cells,[21] podocytes,[22] and glomerular endothelial[23] and mesangial[24] cells. Collectively, these observations suggest that perturbations of the circadian clock in the kidney may influence the development of diabetic hyperglycemia by stimulating renal tubular gluconeogenesis and/or glucose reabsorption, or by acting as a "second hit" contributing to the pathogenesis of DN. To address these hypotheses, we generated and characterized mice with streptozotocin (STZ)-induced type I diabetes and a specific deletion of the circadian clock coordinator *Bmal1* in glomerular podocytes or in the renal tubule.

METHODS

Animals were maintained *ad libitum* on the standard laboratory chow diet (KLIBA NAFAG diet 3800). All experiments were performed on male mice.

Mouse models

Inactivation of the *Bmal1* (*Arntl*) gene was induced by 2-week treatment with doxycycline (DOX; 2 mg/ml in drinking water) of 8-week-old $Bmal1^{lox/lox}$/*Nphs2-rtTA*/LC1 mice (cKOp mice) or of 8-week-old $Bmal1^{lox/lox}$/*Pax8-rtTA*/LC1 mice (cKOt mice). Their littermate controls ($Bmal1^{lox/lox}$ mice) received the same DOX treatment. Both models have been previously described and validated.[6,9] One week after the end of DOX treatment, type I diabetes was induced by i.p. injections of STZ (50 mg/kg body weight [BW]; daily for 5 days). Vehicle-treated mice received vehicle injections of phosphate-buffered saline. All experiments were performed 8 weeks after the last STZ or vehicle injection. In all experiments, tissue and blood collection was performed from mice sacrificed at ZT9 (ZT indicates Zeitgeber time units; ZT0 is the time of light on, and ZT12 is the time of light off).

Metabolic cages

Mice were housed in individual metabolic cages (Tecniplast). Urine collection was performed over 24 hours after a 4-day adaptation period.

Plasma and urine chemistry

Urinary and plasma Na^+, K^+, Ca^{2+}, Mg^{2+}, phosphate, creatinine, glucose, urate, and urea concentrations and osmolality were measured by the Laboratoire de prestations de Chimie Clinique of the Centre Hospitalier Universitaire Vaudois. Urinary pH was assessed with a pH meter (Metrohm). Blood pH and blood gases were measured on mixed arterial-venous blood using an epoc blood analyzer (Siemens Healthcare). Urinary ammonium was measured using the Berthelot method. Urinary titratable acid was measured using the method of Chan.[25] Plasma aldosterone levels were measured by radioimmunoassay (DPC). Plasma insulin was determined using a kit from Mercodia.

GFR

GFR was measured on anesthetized animals with inulin–fluorescein isothiocyanate, as previously described.[26]

I.p. glucose tolerance test

After 15 hours of fasting, vehicle- or STZ-treated control and cKOt mice were i.p. injected with glucose (1 g/kg of BW). Glycemia was measured with glycemia reader in a drop of tail blood (Contour Next One; Bayer) before (time = 0) and 15, 30, 60, 90, 120, and 180 minutes after glucose injection.

Insulin tolerance test

After 4 hours of food restriction, vehicle- or STZ-treated control and cKOt mice were i.p. injected with 0.5 U of insulin (human recombinant insulin; Sigma) per kg of BW. Glycemia was measured before insulin injection (time = 0) and 15, 30, 45, 60, 90, 120, 150, and 180 minutes after insulin injection. If glycemia decreased below 2 mM, mice were rescued by i.p. injection of 30 mg of glucose and were excluded from the analysis.

RNA sequencing

RNA sequencing was performed as described in Ansermet *et al.*[6] *Mus musculus GRCm38* .92 gene annotation was used. Gene counts were scaled using trimmed mean of M values (TMM) normalization and log transformed into counts per million (CPM) using the "cpm" function from the limma R package.[27] Differential expression between knockout and control animals was computed for the untreated

(phosphate-buffered saline) and the treated (STZ) conditions and the interaction between the 2. For each of the 3 comparisons, genes with a false discovery rate (FDR) < 5% were selected for a gene ontology "Biological Process" enrichment analysis with "clusterProfiler."[28] Terms with a Q-value < 0.01 were considered as significant and further processed with the function "simplify" with default parameters to remove redundancy.

Statistical analysis

All data are expressed as mean ± SEM. Statistical tests are described in figure legends and in Supplementary Table S10. $P < 0.05$ was considered significant. Statistical analysis was performed using GraphPad Prism software (version 8.2.1).

Capillary Western blots

Capillary Western blots were performed at the University of Lausanne Protein Analysis Facility (https://www.unil.ch/paf/home/menuinst/technologies/western-in-capillaries.html). Their quantitation was performed in a blinded manner by a technician from this facility.

RESULTS

Inactivation of Bmal1 in podocytes does not lead to induction of DN in STZ-treated mice

Podocyte-specific inactivation of *Bmal1* (*Arntl*) was induced by 2-week treatment with DOX (2 mg/ml in drinking water) of 8-week-old *Bmal1*$^{lox/lox}$/*Nphs2-rtTA*/LC1 mice (hereinafter referred to as cKOp mice).[6] Their littermate controls (*Bmal1*$^{lox/lox}$ mice; hereinafter referred to as control mice) received the same DOX treatment. As shown in Figure 1a, STZ treatment (see Methods) led to hyperglycemia, which was not different between control and cKOp mice. BW was lower in STZ-treated animals, but this effect was similar in mice of both genotypes (Figure 1b). The GFR, measured using inulin–fluorescein isothiocyanate clearance, was not different between STZ-treated control and cKOp mice (Figure 1c). Diabetic animals showed glucosuria (Figure 1d), polyuria (Figure 1e), low-molecular-weight proteinuria (Figure 1f), and slight albuminuria (Figure 1f). However, there was no difference in these parameters between STZ-treated control and cKOp mice.

Mice devoid of BMAL1 in the renal tubule exhibit exacerbated hyperglycemia with diabetes

As shown in Figure 2a, BW was not different in diabetic control mice and mice devoid of BMAL1 in the renal tubule (DOX-treated *Bmal1*$^{lox/lox}$/*Pax8-rtTA*/LC1 mice[9]; hereinafter referred to as cKOt mice). Blood plasma analysis revealed that STZ-induced hyperglycemia is exacerbated in cKOt mice in both fed and fasted conditions (Figure 2b and c, respectively).

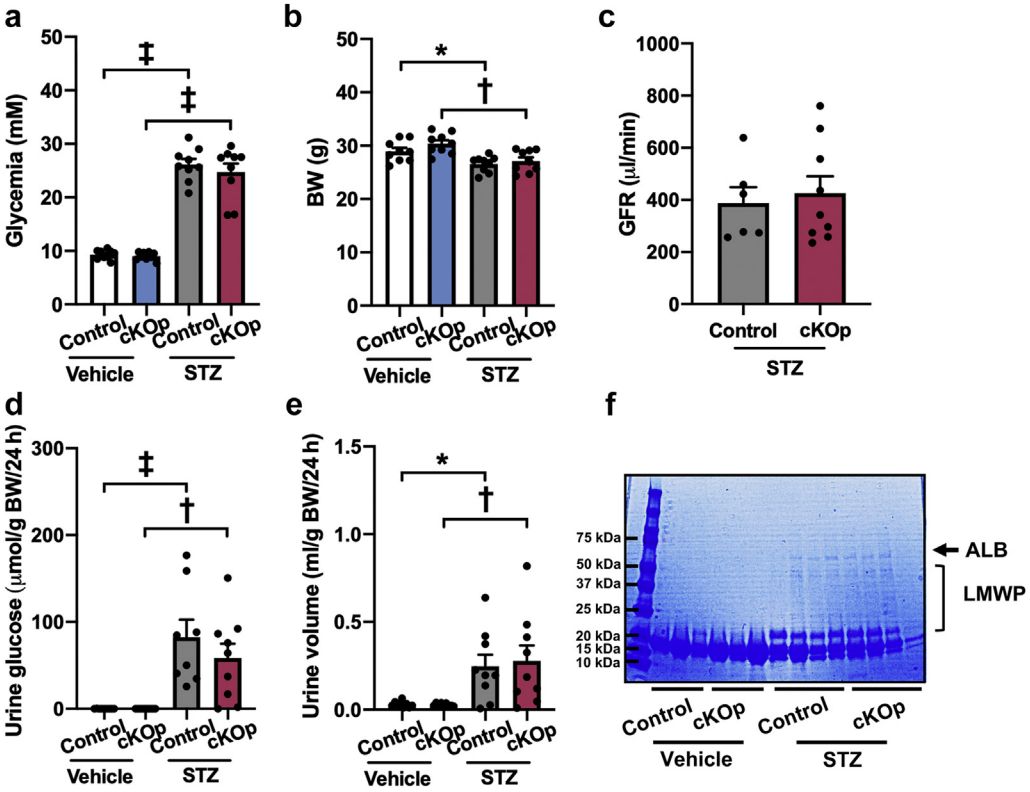

Figure 1 | General characteristics of vehicle- or streptozotocin (STZ)-treated control and cKOp mice. (**a**) Nonfasted glycemia. (**b**) Body weight (BW). (**c**) Glomerular filtration rate (GFR) (inulin clearance). (**d**) Urine glucose. (**e**) Urine volume. (**f**) Coomassie blue staining of urine proteins. For all mice, 0.3% (vol) of 24-hour urine was loaded onto a sodium dodecylsulfate–polyacrylamide gel electrophoresis gel. Means ± SEM are given. n = 9 in each group, except for GFR measurements, where $n = 6$ and $n = 9$ mice were used in STZ-treated control and cKOp groups, respectively. All results were obtained from 19-week-old animals. Two-way analysis of variance with the Sidak multiple comparisons test was used. *$P < 0.05$, †$P < 0.01$, ‡$P < 0.001$. ALB, albumin (65 kDa); LMWP, low-molecular-weight protein.

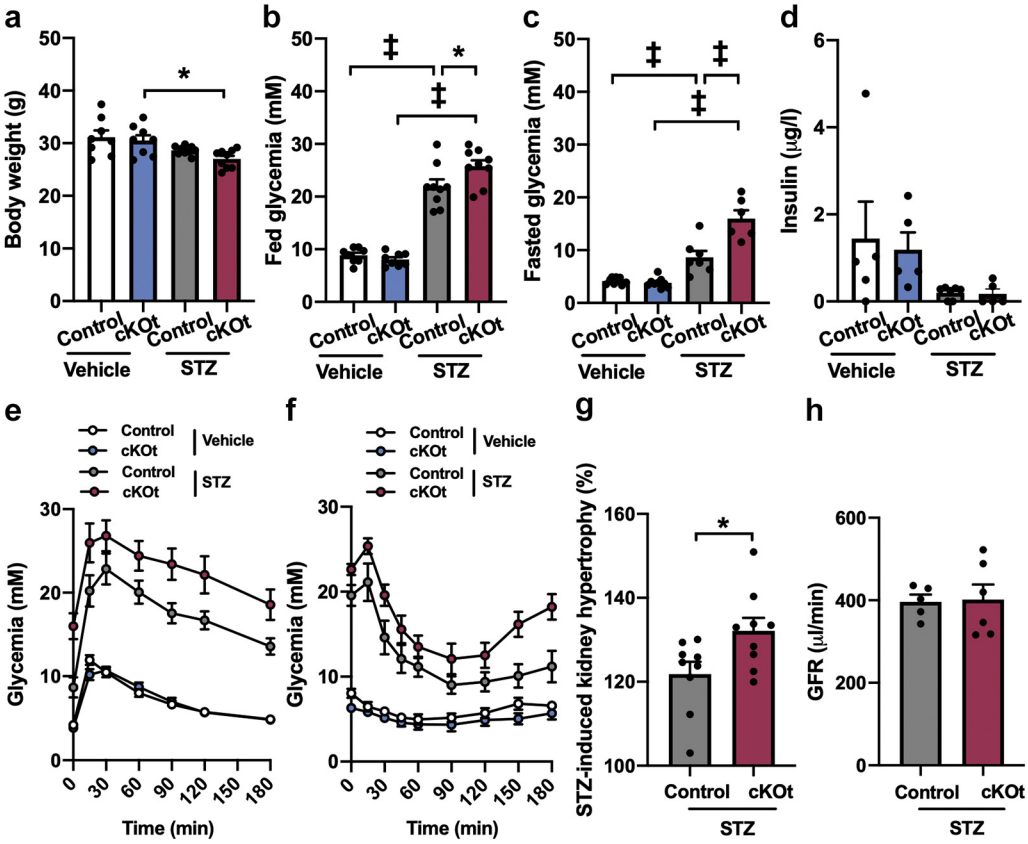

Figure 2 | General characteristics of vehicle- or streptozotocin (STZ)-treated control and cKOt mice. (**a**) Body weight. $n = 8$ for vehicle-treated control and cKOt mice, and $n = 9$ for STZ-treated control and cKOt mice. (**b**) Nonfasted glycemia. $n = 8$ and $n = 9$ for vehicle- and STZ-treated control and cKOt mice, respectively. (**c**) Fasted glycemia (16 hours of fasting). $n = 9$ for vehicle-treated control and cKOt mice, and $n = 7$ and $n = 6$ for STZ-treated control and cKOt mice, respectively. (**d**) Insulin levels in vehicle- or STZ-treated control and cKOt mice. $n = 9$ and $n = 6$ for vehicle-treated control and cKOt mice, respectively, and $n = 10$ and $n = 7$ for STZ-injected control and cKOt mice, respectively. Plasma insulin levels were measured at ZT18, in the middle of the inactive phase. (**e**) Blood glucose levels measured over course of glucose tolerance test in vehicle- or STZ-treated control and cKOt mice. $n = 9$ for vehicle-treated control and cKOt mice, and $n = 7$ and $n = 6$ for STZ-treated control and cKOt mice, respectively. (**f**) Blood glucose levels measured over the course of the insulin tolerance test in vehicle- or STZ-treated control and cKOt mice. $n = 5$ for vehicle- or STZ-treated control mice, and $n = 6$ for vehicle or STZ-treated cKO mice. (**g**) Diabetes-induced kidney hypertrophy. $n = 9$ in each group. Kidney hypertrophy was assessed by dividing kidney weight (KW) with body weight (BW). Relative KW/BW values for STZ-injected control and cKOt animals were calculated by attributing 100% to the corresponding vehicle-injected group. (**h**) Glomerular filtration rate (GFR) (inulin clearance). $n = 5$ and $n = 6$ for STZ-treated control and cKOt mice, respectively. Means ± SEM are given. Two-way analysis of variance with the Sidak multiple comparisons test was used. $^{*}P < 0.05$, $^{\dagger}P < 0.01$, $^{\ddagger}P < 0.001$.

None of the other measured plasma parameters, including osmolality and sodium, potassium, phosphate, calcium, magnesium, creatinine, urate, and aldosterone concentrations, was different between STZ-treated control and cKOt mice, except for increased plasma urea levels in cKOt mice (Supplementary Table S1). Plasma insulin levels were not different between STZ-treated control and cKOt fasted mice (Figure 2d). Glucose and insulin tolerance tests assessed as the slope of the declining glucose concentration did not reveal significant differences between mice of either genotype in both treatment conditions (Figure 2e and f, respectively). Diabetes-induced kidney hypertrophy was more pronounced in diabetic cKOt mice than in diabetic controls (Figure 2g). GFR was not different between STZ-treated mice of both genotypes (Figure 2h). The STZ-induced increase in water intake and urine volume was more pronounced in cKOt mice (Figure 3a and b, respectively), whereas urine osmolality was not different between diabetic mice of both genotypes (Figure 3c). Fractional excretion of glucose was higher and fractional excretion of sodium was lower in STZ-treated cKOt mice compared with STZ-treated controls (Figure 3d and e, respectively), whereas fractional excretion values of phosphate (Figure 3f), magnesium (Figure 3g), and calcium (Figure 3h) were not different between diabetic mice of both genotypes. Both control and cKOt mice treated with STZ had similar low-molecular-weight proteinuria but no albuminuria (Supplementary Figure S1). No major histologic differences were found between kidneys of vehicle- or STZ-treated control and cKOt mice (Supplementary Figure S2).

Exacerbated hyperglycemia in cKOt mice correlates with increased expression of gluconeogenic enzymes in the kidney

To identify molecular pathways associated with exacerbated hyperglycemia in STZ-treated cKOt mice, we performed

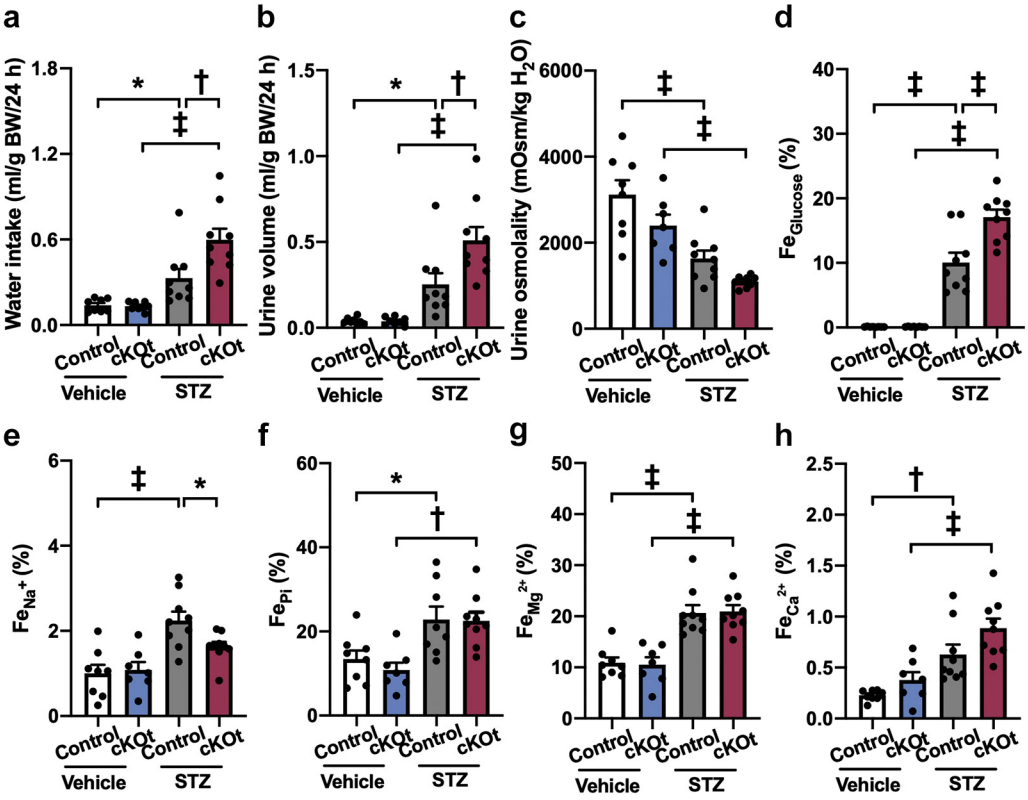

Figure 3 | Water intake and urine characteristics of vehicle- or streptozotocin (STZ)-treated control and cKOt mice. (**a**) The 24-hour water intake. $n = 8$ for vehicle-treated control or cKOt mice, and $n = 9$ for STZ-treated control or cKOt mice. (**b**) The 24-hour urine volume. $n = 8$ for vehicle-treated control or cKOt mice, and $n = 9$ for STZ-treated control or cKOt mice. (**c**) Urine osmolality. $n = 8$ for vehicle-treated control mice, $n = 7$ for vehicle-treated cKOt mice, and $n = 9$ for STZ-treated control or cKOt mice. (**d**) Fractional excretion (Fe) of glucose. $n = 8$ for vehicle-treated control or cKOt mice, and $n = 9$ for STZ-treated control or cKOt mice. (**e**) Fe of sodium. $n = 8$ for vehicle-treated control mice, $n = 7$ for vehicle-treated cKOt mice, and $n = 9$ for STZ-treated control or cKOt mice. (**f**) Fe of phosphate. $n = 8$ for vehicle-treated control mice, $n = 7$ for vehicle-treated cKOt mice, $n = 8$ for STZ-treated control mice, and $n = 9$ for STZ-treated cKOt mice. (**g**) Fe of magnesium. $n = 8$ for vehicle-treated control mice, $n = 7$ for vehicle-treated cKOt mice, and $n = 9$ for STZ-treated control or cKOt mice. (**h**) Fe of calcium. $n = 8$ for vehicle-treated control mice, $n = 7$ for vehicle-treated cKOt mice, and $n = 9$ for STZ-treated control or cKOt mice. Means ± SEM are given. Two-way analysis of variance with the Sidak multiple comparisons test was used. $^{*}P < 0.05$, $^{\dagger}P < 0.01$, $^{\ddagger}P < 0.001$. BW, body weight.

RNA-sequencing analysis of kidney transcriptomes followed by whole-transcriptome pathway enrichment analysis and specific analyses of RNAs encoding proteins involved in renal gluconeogenesis and renal glucose reabsorption. Comparison of transcriptomes revealed 1833 transcripts differentially expressed between vehicle- and STZ-treated controls (Supplementary Table S2; FDR < 5%), 1784 transcripts differentially expressed between vehicle- and STZ-treated cKOt mice (Supplementary Table S3; FDR < 5%), 3107 transcripts differentially expressed between vehicle-treated control and cKOt mice (Supplementary Table S4; FDR < 5%), and 2667 transcripts differentially expressed between STZ-treated control and cKOt mice (Supplementary Table S5; FDR < 5%). Gene ontology analysis of differentially expressed transcripts revealed enrichment of pathways related to lipid, amino acid, and carboxylic acid metabolism, and organic anion transport between control and cKO mice in both vehicle and STZ treatment groups (Figure 4a and b, respectively, and Supplementary Tables S6 and S7, respectively). A total of 284 transcripts exhibited genotype-by-treatment interaction effects (Supplementary Table S8; FDR < 5%), including Glud1 and G6pc transcripts encoding enzymes involved in renal gluconeogenesis (see below). Gene ontology analysis of transcripts with significant interaction showed enrichment of only a limited number of pathways, mainly related to lipid metabolism and organic anion transport (Figure 4c and Supplementary Table S9). Among the genes encoding transporters involved in glucose reabsorption in the proximal tubule (*Sglt1*, *Sglt2*, *Glut1*, and *Glut2*), only *Glut1* (*Slc2a1*) displayed higher expression in kidneys of diabetic cKOt mice compared with diabetic controls (Supplementary Table S5).

The 2 main gluconeogenic precursors in the kidney are lactate and glutamine.[29] As shown in Figure 4d and e and Supplementary Table S5, expression levels of transcripts encoding proteins involved in renal glutamine gluconeogenesis (Snat3, Gls, and Glud1) were increased in kidneys of STZ-treated cKOt mice compared with STZ-treated controls. Conversely, expression of the mRNA encoding glutamate-ammonia ligase (GLUL), which reverses the GLS-driven

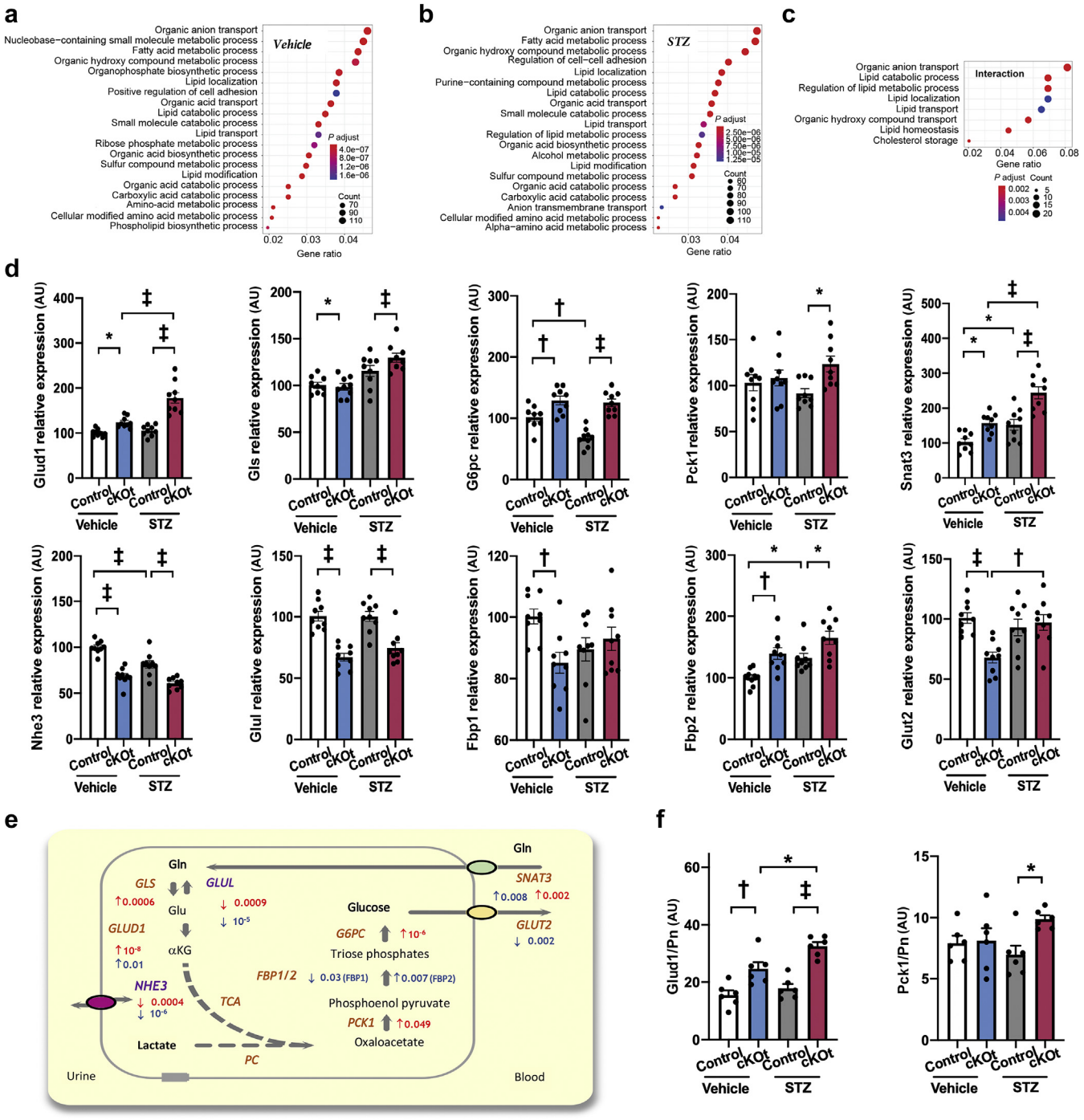

Figure 4 | Gene ontology (GO) "Biological Process" enrichment analysis. (**a**) GO analysis of transcripts differentially expressed in kidneys of vehicle-treated control and cKOt mice. (**b**) GO analysis of transcripts differentially expressed in kidneys of streptozotocin (STZ)-treated control and cKOt mice. (**c**) GO analysis of transcripts exhibiting genotype-by-treatment interaction effect. Dot plots for the top 20 most significant terms (Q value < 0.01). Redundant terms were filtered. GeneRatio represents the fraction of significant genes annotated with the term displayed. The size of the dot represents the number of significant genes annotated with the term displayed. $n = 6$ per condition. (**d**) Fold-change plots for transcripts encoding enzymes and transcripts involved in renal gluconeogenesis. The expression level values were extracted from Supplementary Tables S2, S3, S4, and S5. $^{*}P < 0.05$, $^{\dagger}P < 0.01$, $^{\ddagger}P < 0.001$. (**e**) Schematic representation of proximal tubule cells with principal proteins/enzymes involved in the process of renal gluconeogenesis. In red: P values for differential expression between STZ-treated control and cKOt mice. In blue: P values for differential expression between vehicle-treated control and cKOt mice. Red and blue arrows indicate increased (↑) or decreased (↓) expression in cKOt mice. (**f**) Quantitative analysis of capillary Western blots for glutamate dehydrogenase (GLUD1) and phosphoenolpyruvate carboxykinase (PCK1; Supplementary Figures S2 and S3, respectively) in kidneys from phosphate buffered saline– or STZ-treated control and cKOt mice ($n = 6$ per condition). Two-way analysis of variance with the Sidak multiple comparisons test was used. $^{*}P < 0.05$, $^{\dagger}P < 0.01$, $^{\ddagger}P < 0.001$. AU, arbitrary unit; FBP1/2, fructose-1,6-biphosphatase 1/2; G6PC, glucose-6-phosphatase; GLS, glutaminase; GLUL, glutamine synthetase; GLUT2, glucose transporter 2; NHE3, sodium-hydrogen exchanger 3; P adjust, P adjusted; PC, pyruvate carboxylase; SNAT3, glutamine transporter; TCA, tricarboxylic acid cycle.

initial step of glutaminolysis, was decreased. Similarly, expression levels of mRNAs encoding 2 enzymes in the common part of the gluconeogenic pathway (namely, phosphoenolpyruvate carboxykinase [Pck1] and glucose-6-phosphatase [G6pc]), were higher in STZ-treated cKOt mice. Higher expression of GLUD1 and PCK1 in kidneys of diabetic cKOt mice was confirmed at the protein level by capillary Western blot (Figure 4f and Supplementary Figure S3). In the liver of diabetic mice, the expression level of GLUD1 was not different between control and cKOt mice, and expression of PCK1 was lower in cKOt mice (Supplementary Figure S4). Of note, expression levels of Glud1, Snat3, fructose-1,6-biphospatase 2 (Fbp2), and Glut1 were higher and expression levels of Glul, Fbp1, and Glut2 were lower in kidneys of vehicle-treated cKOt mice compared with vehicle-treated controls.

Multiple mechanisms directly or indirectly affecting the gluconeogenic pathway are changed in kidneys of diabetic cKOt mice

The gluconeogenic pathway in the kidney can be influenced by the circadian clock either directly, through transcriptional, translational, or posttranslational control of proteins involved in renal gluconeogenesis, or indirectly, by affecting other renal mechanisms that are intrinsically connected to glucose production in the proximal tubule. Transcriptional factors, coactivators, and corepressors that govern transcription of gluconeogenic enzymes have been partially characterized in liver, kidney, and other tissues. Figure 5a and b summarize changes in expression levels of transcripts encoding known transcriptional regulators of gluconeogenesis in kidneys of control and cKOt mice (see also Supplementary Tables S4 and S5). Among the analyzed transcripts, those encoding peroxisome proliferator-activated receptor δ (PPARδ) and cryptochromes 1 and 2 showed a substantial increase, whereas nuclear receptor NR1D1 (also known as REV-ERBα) was substantially decreased in kidneys of cKOt mice in both vehicle- and STZ-treated animals compared with controls with the same treatment. Expression of peroxisome proliferator-activated receptor γ coactivator 1-α (Pgc1α, Ppargc1a) was increased in STZ-treated cKOt mice compared with STZ-treated controls, and expression of glucocorticoid receptor (Gr, Nr3c1) was decreased in vehicle-treated cKOt

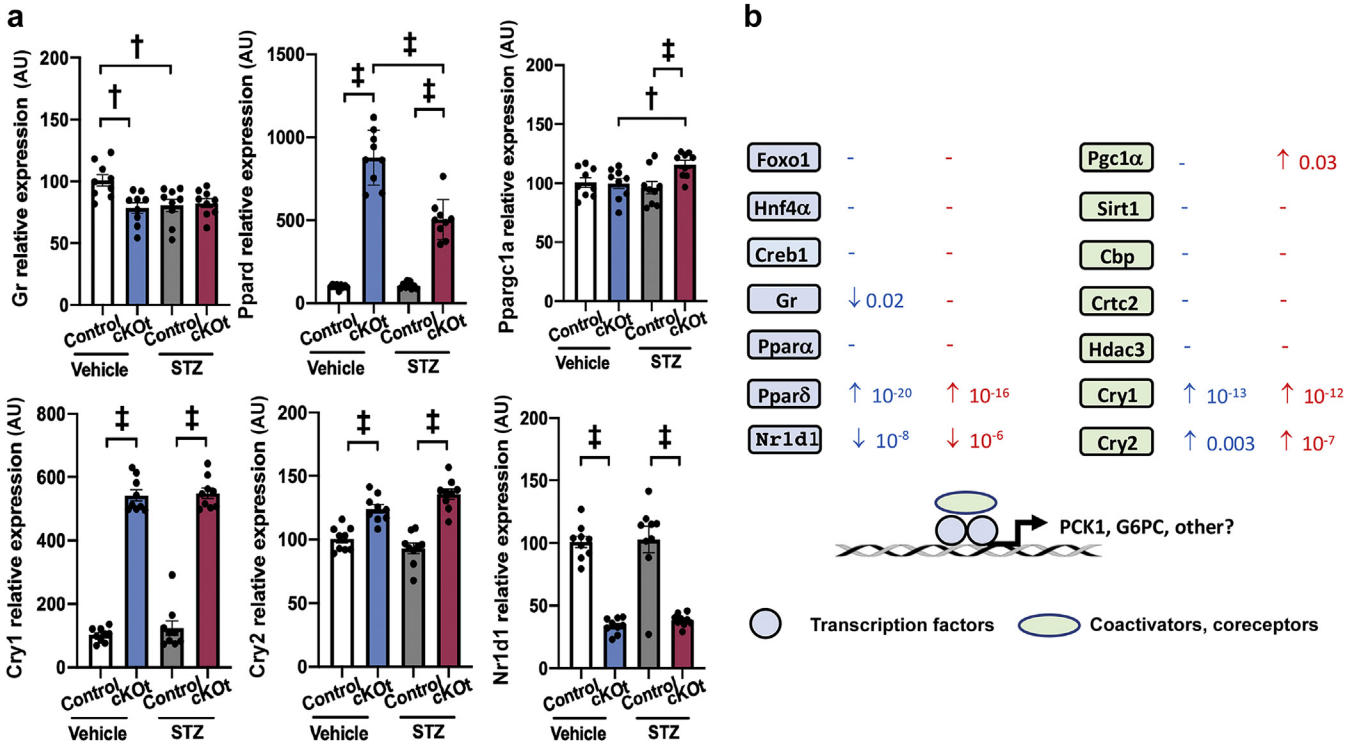

Figure 5 | (a) Fold-change plots for transcripts encoding transcription factors, coactivators, and corepressors that govern transcription of gluconeogenic enzymes in vehicle- and streptozotocin (STZ)-treated control and cKOt mice. The expression level values were extracted from Supplementary Tables S2, S3, S4, and S5. *$P < 0.05$, †$P < 0.01$, ‡$P < 0.001$. (**b**) Schematic representation of data presented in Figure 5a. In red: *P* values for differential expression between STZ-treated control and cKOt mice. In blue: *P* values for differential expression between vehicle-treated control and cKOt mice. Red and blue arrows indicate increased (↑) or decreased (↓) expression in cKOt mice. AU, arbitrary unit; Cbp, CREB-binding protein; Creb1, cyclic adenosine monophosphate responsive element binding protein; Crtc2, CREB-regulated transcriptional coactivator 2; Cry1, cryptochrome circadian regulator 1; Cry2, cryptochrome circadian regulator 2; Foxo1, forkhead O box protein; G6PC, glucose 6-phosphatase; Gr, glucocorticoid receptor; Hdac3, histone deacetylase 3; Hnf4α, hepatocyte nuclear factor 4 α; Nrld1, nuclear receptor subfamily 1 group D member 1; Pgc1α, peroxisome proliferator-activated receptor γ coactivator 1-α; PCK1, phosphoenolpyruvate carboxykinase 1; Pparα, peroxisome proliferator-activated receptor α; Pparδ, peroxisome proliferator-activated receptor δ; Sirt1, NAD-dependent deacetylase sirtuin-1.

mice compared with vehicle-treated controls. Expression of forkhead O box protein (Foxo1), hepatocyte nuclear factor 4 α (Hnf4a), cyclic adenosine monophosphate responsive element binding protein (Creb1), Pparα, Sirt1, CREB-binding protein (Cbp, Crebbp), CREB-regulated transcriptional coactivator 2 (Crtc2), and histone deacetylase 3 (Hdac3) was unaffected by treatment or genotype.

Because acidosis is the major indirect stimulus for renal gluconeogenesis, we measured blood and urinary pH, blood gases, urinary excretion of ammonia (NH_3/NH_4^+), and titratable acidity. As shown in Figure 6, blood pH was higher in vehicle-treated cKOt mice compared with vehicle-treated controls but was not different between diabetic mice of both genotypes. Plasma bicarbonate was lower in diabetic controls compared with vehicle-treated controls; however, no difference was found in plasma bicarbonate between diabetic control and cKOt mice. Plasma base excess and urine pH were not affected by treatment or genotype. However, the STZ-treated cKOt mice excreted increased amounts of ammonia and titratable acidity compared with STZ-treated controls. Analysis of transcripts encoding proteins involved in renal acid–base handling revealed decreased expression of sodium-hydrogen exchanger NHE3 (Slc9a3; see Figure 4d and e) and of anion exchanger AE1 (Slc4a1) and increased expression of carbonic anhydrase II (Car2) and b1 subunit of H^+-ATPase (Atp6v1b1). However, no difference was observed in expression levels of chloride-proton antiporter Clcn5, b2 subunit of H^+-ATPase (Atp6v1b2), ammonia transporter Rhcg, sodium-bicarbonate cotransporter NBCE1 (Slc4a4), sodium-dependent chloride-bicarbonate exchanger NDCBE (Slc4a8), and anion exchanger pendrin (Pds, Slc26a4) in diabetic cKOt mice compared with diabetic controls (Supplementary Table S5). Of note, expression levels of Nhe3 were lower in kidneys of vehicle-treated cKOt mice compared with vehicle-treated controls (Figure 4d and Supplementary Table S4).

DISCUSSION

It is well established that dysfunction of the circadian clock mechanism or a misalignment between the biological clock and social and environmental cues caused (e.g., by shift work) computer/internet addiction, frequent jetlag, or sleep disorders, are major risk factors for pathogenesis and/or progression of a variety of chronic diseases. However, the contribution of tissue-intrinsic local circadian clocks versus systemic circadian cues to specific pathophysiological processes has not been widely investigated. We hypothesized that perturbations in intrinsic renal circadian clocks may contribute to the development of DN and/or diabetic hyperglycemia. To test these hypotheses, we used 2 mouse models (i.e., cKOp and cKOt mice) developed on a C57BL/6 genetic background known to be relatively resistant to DN. In both models, deficiency in BMAL1 in diabetic conditions did not result in additional albuminuria or difference in GFR, 2

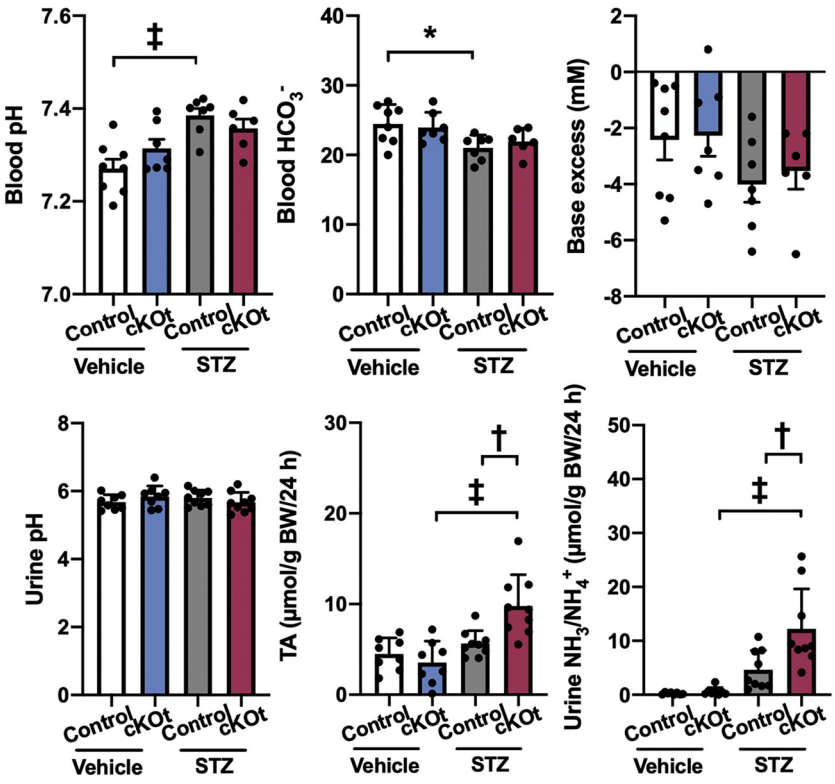

Figure 6 | Plasma pH, plasma bicarbonate, plasma base excess, urine pH, 24-hour urine titratable acidity (TA), and ammonium excretion in vehicle- or streptozotocin (STZ)-treated control and cKOt mice. $n = 6–9$. Two-way analysis of variance with the Sidak multiple comparisons test was used. $^*P < 0.05$, $^\dagger P < 0.01$, $^\ddagger P < 0.001$.

major hallmarks of the disease. This either suggests that transgenic mice on a C57BL/6 background may not be an appropriate model to study the "second-hit" hypothesis in DN or that pathogenesis and/or progression of DN are more affected by systemic circadian perturbations rather than by intrinsic renal circadian clocks. Testing the hypothesis of an interaction between diabetic hyperglycemia and intrinsic renal circadian clocks revealed enhanced renal tubular gluconeogenic pathway and exacerbated hyperglycemia in diabetic cKOt mice. mRNA and protein expression analyses indicated that both glutamine gluconeogenesis and the common part of the gluconeogenic pathway are enhanced in diabetic cKOt mice compared with diabetic controls. This observation suggested that both principal gluconeogenic substrates in the kidney (i.e., glutamine and lactate) could contribute to the worsening of hyperglycemia in cKOt mice.

Kidney gluconeogenesis has gained increased interest in recent years because of the potentially important role of glucose produced in the renal tubule in both systemic metabolic balance and kidney disease (reviewed previously[2,30]). The kidney accounts for 40% of overall body *de novo* glucose production in overnight fasted humans.[29] In diabetes, both liver and kidney increase glucose synthesis, but the relative increase in renal gluconeogenesis is much stronger than in the liver. Studies in the liver have shown that the circadian clock can influence hepatic gluconeogenesis via multiple circadian clock-controlled cellular mechanisms. Zhang *et al.* have shown that circadian repressors cryptochromes 1 and 2 inhibit expression of gluconeogenic enzymes by blocking cyclic adenosine monophosphate–dependent activation of CREB1.[31] Li *et al.* have demonstrated that NR1D1, which forms a critical negative limb in the core circadian clock, supresses transcription of Pck1 and G6pc.[32] As expected for circadian clock genes in *Bmal1* knockout mice,[33] our results demonstrated a strong upregulation of Cry1/Cry2 transcripts and a strong downregulation of Nr1d1 transcript in kidneys of diabetic cKOt mice compared with diabetic controls. These contradictory results may suggest tissue specificity of gluconeogenesis regulation by the core clock elements. Interestingly, kidneys of diabetic cKOt mice exhibited a strong induction of Pparδ, which has been shown to dramatically stimulate Pck1 expression in muscle.[34] Finally, expression of the mRNA encoding PGC1α, a critical coactivator of FoxO1, a transcriptional factor that controls expression of gluconeogenic enzymes in both kidney and liver, was increased in the kidneys of diabetic cKOt mice. Collectively, analysis of renal transcriptomes revealed that diabetic cKOt mice exhibit substantial changes in several cellular pathways involved in the control of gluconeogenesis in the kidney and/or other tissues.

Assessment of potential mechanisms through which the circadian clock may influence the gluconeogenic pathway in the diabetic kidney revealed several features of compensated blood acid–base status, including increased urinary excretion of ammonium and titratable acidity. These observations paralleled transcriptomics data that demonstrated a reduction in expression levels of the transcript encoding NHE3, a transporter that plays a key role in proximal tubule acid–base handling, along with a potentially compensatory increase in the expression of the gene encoding ATP6V1B1 subunit of H^+-ATPase involved in H^+ secretion in the distal nephron. Direct control of Nhe3 expression by the circadian clock has been demonstrated at both the transcriptional[16] and protein expression level.[35] Thus, intracellular acidification due to reduced NHE3 expression could be considered as a possible cause of increased gluconeogenesis in proximal tubule cells of cKOt mice. These results parallel findings by Onishi *et al.*,[36] who demonstrated that tubule-specific knockout of NHE3 results in the increased expression of gluconeogenic enzymes in the kidney. Enhancement of rate-limiting common part of the gluconeogenic pathway (PCK1 and G6PC) in diabetic cKOt mice may further aggravate the intracellular acidification via the enhancement of glutamine gluconeogenesis, a metabolic process that generates hydrogen ions. Interestingly, expression of Nhe3, Glul, Glud1, and Snat3, as well as of several transcripts encoding transcription factors, coactivators, or corepressors that govern transcription of gluconeogenic enzymes (Gr, Pparδ, Nr1d1, Cry1, and Cry2) was modified in a similar manner in STZ- and vehicle-treated cKOt mice. This suggests that renal gluconeogenesis is also enhanced in vehicle-treated cKOt mice. In nondiabetic conditions, the absence of hyperglycemia in cKOt mice could be plausibly explained by increased metabolism of this excessively synthesized glucose by all glucose-metabolizing tissues, including the kidney.

What is the relevance of these findings to the pathogenesis of diabetes in humans? It is well established that feeding rhythm plays an important role in the entrainment of peripheral circadian clocks.[37] Food components (e.g., high salt,[38] low-carbohydrate high-protein diet,[39] and ketogenic diet[40]) and food intake-driven paracrine/autocrine factors (e.g., corticosteroids[41]) have been shown to have a strong impact on circadian rhythms in the kidney. Several major population groups are periodically or constantly exposed to shifted or disordered food intake. For instance, up to ∼20% to 25% of North America and European employees perform shift work, which is associated with an altered feeding pattern.[42] The second rapidly growing group with affected dietary behavior is severe internet addicts, which represent, according to current estimates, 6% to 8% of the general population.[43] Sleep disorders,[44] chronic kidney disease,[45] and some medications (e.g., cisplatin[46]) have also been shown to significantly impair renal circadian rhythms. Thus, one may speculate that in a substantial fraction of diabetic patients, hyperglycemia may be further worsened due to dysregulation of circadian clocks in peripheral tissues, including intrinsic renal circadian clocks. Along these lines, a large number of studies have demonstrated a strong association between shift work and the risk to develop diabetes (reviewed previously[47]). Collectively, our results provide a new molecular link between the circadian system and pathophysiology of diabetes.

DISCLOSURE

All the authors declared no competing interests.

ACKNOWLEDGMENTS

This work was supported by the Swiss National Science Foundation research grant 310030-188499 (to DF) A part of this work has been submitted as an abstract to the 2021 Annual Meeting of the American Society of Nephrology.

AUTHOR CONTRIBUTIONS

HAIY, FG, and DF designed the study; CA, GC, DO, YB, and AG performed experiments; CA, GC, DO, SP, LM, and HAIY analyzed the data; CA and HAIY made the figures; DF and HAIY wrote the manuscript. All authors approved the final version of the manuscript.

SUPPLEMENTARY MATERIAL

Supplementary File (PDF)

Figure S1. Coomassie blue staining of urine proteins from vehicle- or streptozotocin (STZ)-treated control and cKOt mice.

Figure S2. (**A**) Masson trichrome staining of kidney sections from vehicle- or streptozotocin (STZ)-treated control and cKOt mice. (**B**) Periodic acid–Schiff (PAS) staining of kidney sections from vehicle- or streptozotocin (STZ)-treated control and cKOt mice.

Figure S3. Capillary Western blot analysis of glutamate dehydrogenase 1 (GLUD1; **A**) and phosphoenolpyruvate carboxykinase (PCK1; **B**) expression in kidneys of vehicle- or streptozotocin (STZ)-treated control and cKOt mice.

Figure S4. Capillary Western blot analysis of glutamate dehydrogenase 1 (GLUD1; **A**) and phosphoenolpyruvate carboxykinase (PCK1; **B**) expression in the liver of vehicle- or streptozotocin (STZ)-treated control and cKOt mice.

Table S1. Plasma chemistry in vehicle- or streptozotocin (STZ)-injected control and cKOt mice.

Supplementary Files (Excel)

Table S2. Transcriptome: control streptozotocin (STZ) versus control phosphate-buffered saline (PBS).

Table S3. Transcriptome: knockout (KO) streptozotocin (STZ) versus KO phosphate-buffered saline (PBS).

Table S4. Transcriptome: knockout (KO) phosphate-buffered saline (PBS) versus control PBS.

Table S5. Transcriptome: knockout (KO) streptozotocin (STZ) versus control STZ.

Table S6. Gene ontology (GO) enrichment for knockout (KO) phosphate-buffered saline (PBS) versus control PBS.

Table S7. Gene ontology (GO) enrichment for knockout (KO) streptozotocin (STZ) versus control STZ.

Table S8. Transcriptome: genotype-by-treatment interaction.

Table S9. Gene ontology (GO) enrichment for interaction.

Table S10. Statistics.

REFERENCES

1. Vallon V. Glucose transporters in the kidney in health and disease. *Pflugers Arch*. 2020;472:1345–1370.
2. Gerich JE. Role of the kidney in normal glucose homeostasis and in the hyperglycaemia of diabetes mellitus: therapeutic implications. *Diabet Med*. 2010;27:136–142.
3. Mithieux G, Gautier-Stein A, Rajas F, et al. Contribution of intestine and kidney to glucose fluxes in different nutritional states in rat. *Comp Biochem Physiol B Biochem Mol Biol*. 2006;143:195–200.
4. Gheith O, Farouk N, Nampoory N, et al. Diabetic kidney disease: world wide difference of prevalence and risk factors. *J Nephropharmacol*. 2016;5:49–56.
5. Firsov D, Bonny O. Circadian rhythms and the kidney. *Nat Rev Nephrol*. 2018;14:626–635.
6. Ansermet C, Centeno G, Nikolaeva S, et al. The intrinsic circadian clock in podocytes controls glomerular filtration rate. *Sci Rep*. 2019;9:16089.
7. Stow LR, Richards J, Cheng KY, et al. The circadian protein period 1 contributes to blood pressure control and coordinately regulates renal sodium transport genes. *Hypertension*. 2012;59:1151–1156.
8. Zuber AM, Centeno G, Pradervand S, et al. Molecular clock is involved in predictive circadian adjustment of renal function. *Proc Natl Acad Sci U S A*. 2009;106:16523–16528.
9. Nikolaeva S, Ansermet C, Centeno G, et al. Nephron-specific deletion of circadian clock gene Bmal1 alters the plasma and renal metabolome and impairs drug disposition. *J Am Soc Nephrol*. 2016;27:2997–3004.
10. Tokonami N, Mordasini D, Pradervand S, et al. Local renal circadian clocks control fluid-electrolyte homeostasis and BP. *J Am Soc Nephrol*. 2014;25:1430–1439.
11. Motohashi H, Tahara Y, Whittaker DS, et al. The circadian clock is disrupted in mice with adenine-induced tubulointerstitial nephropathy. *Kidney Int*. 2020;97:728–740.
12. Charles LE, Gu JK, Fekedulegn D, et al. Association between shiftwork and glomerular filtration rate in police officers. *J Occup Environ Med*. 2013;55:1323–1328.
13. Boogaard PJ, Caubo ME. Increased albumin excretion in industrial workers due to shift work rather than to prolonged exposure to low concentrations of chlorinated hydrocarbons. *Occup Environ Med*. 1994;51:638–641.
14. Kim SJ, Kim JW, Cho YS, et al. Influence of circadian disruption associated with artificial light at night on micturition patterns in shift workers. *Int Neurourol J*. 2019;23:258–264.
15. Uhm JY, Kim HR, Kang GH, et al. The association between shift work and chronic kidney disease in manual labor workers using data from the Korea National Health and Nutrition Examination Survey (KNHANES 2011-2014). *Ann Occup Environ Med*. 2018;30:69.
16. Solocinski K, Richards J, All S, et al. Transcriptional regulation of NHE3 and SGLT1 by the circadian clock protein Per1 in proximal tubule cells. *Am J Physiol Renal Physiol*. 2015;309:F933–F942.
17. Wolf G. Cell cycle regulation in diabetic nephropathy. *Kidney Int Suppl*. 2000;77:S59–S66.
18. Papadimitriou A, Silva KC, Peixoto EB, et al. Theobromine increases NAD(+)/Sirt-1 activity and protects the kidney under diabetic conditions. *Am J Physiol Renal Physiol*. 2015;308:F209–F225.
19. Perelis M, Ramsey KM, Bass J. The molecular clock as a metabolic rheostat. *Diabetes Obes Metab*. 2015;17(suppl 1):99–105.
20. Ramanathan C, Kathale ND, Liu D, et al. mTOR signaling regulates central and peripheral circadian clock function. *PLoS Genet*. 2018;14:e1007369.
21. Sakaguchi M, Isono M, Isshiki K, et al. Inhibition of mTOR signaling with rapamycin attenuates renal hypertrophy in the early diabetic mice. *Biochem Biophys Res Commun*. 2006;340:296–301.
22. Godel M, Hartleben B, Herbach N, et al. Role of mTOR in podocyte function and diabetic nephropathy in humans and mice. *J Clin Invest*. 2011;121:2197–2209.
23. Lenoir O, Jasiek M, Henique C, et al. Endothelial cell and podocyte autophagy synergistically protect from diabetes-induced glomerulosclerosis. *Autophagy*. 2015;11:1130–1145.
24. Lu Q, Zhou Y, Hao M, et al. The mTOR promotes oxidative stress-induced apoptosis of mesangial cells in diabetic nephropathy. *Mol Cell Endocrinol*. 2018;473:31–43.
25. Chan JC. The rapid determination of urinary titratable acid and ammonium and evaluation of freezing as a method of preservation. *Clin Biochem*. 1972;5:94–98.
26. Eisner C, Faulhaber-Walter R, Wang Y, et al. Major contribution of tubular secretion to creatinine clearance in mice. *Kidney Int*. 2010;77:519–526.
27. Ritchie ME, Phipson B, Wu D, et al. limma powers differential expression analyses for RNA-sequencing and microarray studies. *Nucleic Acids Res*. 2015;43:e47.
28. Yu G, Wang LG, Han Y, et al. clusterProfiler: an R package for comparing biological themes among gene clusters. *Omics*. 2012;16:284–287.
29. Gerich JE, Meyer C, Woerle HJ, et al. Renal gluconeogenesis: its importance in human glucose homeostasis. *Diabetes Care*. 2001;24:382–391.
30. Legouis D, Faivre A, Cippà PE, et al. Renal gluconeogenesis: an underestimated role of the kidney in systemic glucose metabolism. *Nephrol Dial Transplant*. Published online November 28, 2020. https://doi.org/10.1093/ndt/gfaa302.
31. Zhang EE, Liu Y, Dentin R, et al. Cryptochrome mediates circadian regulation of cAMP signaling and hepatic gluconeogenesis. *Nat Med*. 2010;16:1152–1156.

32. Li X, Xu M, Wang F, et al. Interaction of ApoA-IV with NR4A1 and NR1D1 represses G6Pase and PEPCK transcription: nuclear receptor-mediated downregulation of hepatic gluconeogenesis in mice and a human hepatocyte cell line. *PLoS One*. 2015;10:e0142098.
33. Weger BD, Gobet C, David FPA, et al. Systematic analysis of differential rhythmic liver gene expression mediated by the circadian clock and feeding rhythms. *Proc Natl Acad Sci U S A*. 2021;118:e2015803118.
34. Fan W, Waizenegger W, Lin CS, et al. PPARδ promotes running endurance by preserving glucose. *Cell Metab*. 2017;25:1186–1193. e1184.
35. Saifur Rohman M, Emoto N, Nonaka H, et al. Circadian clock genes directly regulate expression of the Na(+)/H(+) exchanger NHE3 in the kidney. *Kidney Int*. 2005;67:1410–1419.
36. Onishi A, Fu Y, Darshi M, et al. Effect of renal tubule-specific knockdown of the Na(+)/H(+) exchanger NHE3 in Akita diabetic mice. *Am J Physiol Renal Physiol*. 2019;317:F419–F434.
37. Schibler U, Ripperger J, Brown SA. Peripheral circadian oscillators in mammals: time and food. *J Biol Rhythms*. 2003;18:250–260.
38. Speed JS, Hyndman KA, Roth K, et al. High dietary sodium causes dyssynchrony of the renal molecular clock in rats. *Am J Physiol Renal Physiol*. 2018;314:F89–F98.
39. Oishi K, Uchida D, Itoh N. Low-carbohydrate, high-protein diet affects rhythmic expression of gluconeogenic regulatory and circadian clock genes in mouse peripheral tissues. *Chronobiol Int*. 2012;29:799–809.
40. Oishi K, Uchida D, Ohkura N, et al. Ketogenic diet disrupts the circadian clock and increases hypofibrinolytic risk by inducing expression of plasminogen activator inhibitor-1. *Arterioscler Thromb Vasc Biol*. 2009;29:1571–1577.
41. Sujino M, Furukawa K, Koinuma S, et al. Differential entrainment of peripheral clocks in the rat by glucocorticoid and feeding. *Endocrinology*. 2012;153:2277–2286.
42. Souza RV, Sarmento RA, de Almeida JC, et al. The effect of shift work on eating habits: a systematic review. *Scand J Work Environ Health*. 2019;45:7–21.
43. Kim Y, Park JY, Kim SB, et al. The effects of internet addiction on the lifestyle and dietary behavior of Korean adolescents. *Nutr Res Pract*. 2010;4:51–57.
44. Canales MT, Holzworth M, Bozorgmehri S, et al. Clock gene expression is altered in veterans with sleep apnea. *Physiol Genomics*. 2019;51:77–82.
45. Egstrand S, Olgaard K, Lewin E. Circadian rhythms of mineral metabolism in chronic kidney disease-mineral bone disorder. *Curr Opin Nephrol Hypertens*. 2020;29:367–377.
46. Cao BB, Li D, Xing X, et al. Effect of cisplatin on the clock genes expression in the liver, heart and kidney. *Biochem Biophys Res Commun*. 2018;501:593–597.
47. Schilperoort M, Rensen PCN, Kooijman S. Time for novel strategies to mitigate cardiometabolic risk in shift workers. *Trends Endocrinol Metab*. 2020;31:952–964.